Theoretical Study of β-Peptide Models: Intrinsic Preferences of Helical Structures

by **Yun-Dong Wu***, **Jin-Qiu Lin**, and **Yi-Lei Zhao**

Department of Chemistry, The Hong Kong University of Science and Technology, Clear Water Bay, Kowloon, Hong Kong, China

Dedicated to Professor *Dieter Seebach* on the occasion of his 65th birthday

β-Peptides form various secondary structures, such as *14*-helix, *12*-helix, *10*/*12*-helix, *10*-helix, 2_8-ribbon, *C6*-ribbon, and pleated-sheet. Thus, it is useful to understand the intrinsic backbone conformational preferences of these basic structures. By using a simple repeating-unit method, we have calculated the preferences of *C6*-ribbon, β-strand, *10*/*12*-helix, *14*-helix, *12*-helix, *10*-helix, and 2_8-ribbon of a series of poly-β-alanine models, Ac-(β-Ala)$_n$-NH$_2$, with $n = 1-9$. Interactions among single amino acids result in cooperative residue energies. This is not found for the formations of β-strands, 2_8-ribbons, and *C6*-ribbons, which possess constant residue energies. In contrast, the *12*-helix, *10*-helix, and *14*-helix are characterized by increasing residue energies as the peptide elongates. Therefore, there is a considerable positive cooperative impetus in the gas phase for their formation. The residue energy of the *10*/*12*-helix increases significantly for $n = 2$ and *3*, and then displays a zigzag pattern. Meanwhile, there is a good correlation between calculated residue energies and residue dipole moments, indicating the importance of long-range electrostatic interactions to the cooperative residue energy. Efforts have been made to separate the electrostatic and torsional interactions between residues. Thereby, the *12*-, *10*-, and *10*/*12*-helices all benefit from electrostatic interactions, while the 14-helix has the most intrinsic preference in terms of torsional interaction. The effect of MeOH on the secondary structures has also been evaluated by SCIPCM solvent model calculations.

1. Introduction. – The discovery of *Seebach* and *Gellman* and co-workers that β-peptides readily form various secondary structures, *e.g.*, *14*-helix, *12*-helix, *10*/*12*-helix, *10*-helix, 2_8-ribbon, turns, and pleated-sheets [1–6], has generated tremendous excitement [7]. Since β-amino acids usually possess two stereogenic centers, a large number of structural variations are possible, which makes them interesting building blocks in molecular design [8]. According to circular dichroism (CD) spectra, some β-peptides appear to possess unknown secondary structures that still need to be solved [9]. Another feature of β-peptides is their resistance to enzymatic degradation [10], which is important for pharmaceutically active agents. Indeed, several β-peptides have been found to display biological activity against, *e.g.*, HIV [11], cancer [12], and bacteria [13]. The incorporation of a piece of a synthetic β-peptide into a natural peptide has been found not only to increase the stability of the latter, but also to enhance its protein binding ability [14].

The conformational features of β-peptides have recently been explored by both *ab initio* quantum-mechanical calculations and molecular dynamics simulations [15–20]. *Hoffman* and ourselves have studied the conformations of dipeptide models [13][14] that tend to adopt various folded conformations, with a gauche dihedral angle μ (*cf.* **A** for definition). This property seems to be important for the stabilization of helical

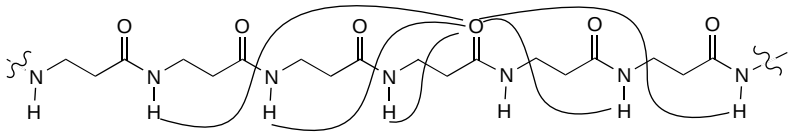

14-Helix *10*-Helix *C6*-Ribbon 2_8-Ribbon *12*-Helix

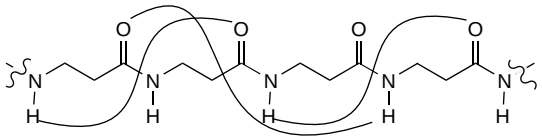

10/*12*-Helix

structures. We have also studied several β-hexapeptide model compounds and found that there is an intrinsic preference for the *10*/*12*-helix over the *14*-helix both in the gas phase and in MeOH solution, provided there is no side chain [17]. Substituent effects on the relative stabilities of *14*- and *10*/*12*-helices have also been explored, and some qualitative predictions about secondary structures can be made. *Van Gunsteren* and *Aqvist* have applied molecular dynamics simulations to explore the folding-unfolding thermodynamics of β-peptides [18][19]. These simulations not only indicate that the experimentally observed helical structures can be easily formed, they also provided detailed information about the process of folding and unfolding. It was found that simulations are quite sensitive to the inclusion of long-range electrostatic interactions [18][19]. *Christianson et al.* also studied the folding process of β-peptides made of *trans*-2-aminocyclopentanecarboxylic acid and *trans*-2-aminocyclohexane carboxylic acid derivatives by using a modified AMBER force field [20].

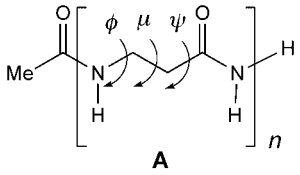

A

n = 0 – 9 (repeating units)

Despite many efforts, several theoretical issues still need to be resolved: *1*) what is the origin of the stability of these helical structures?, *2*) what are the detailed electronic and steric interactions among the amino acid residues?, *3*) is there cooperative interaction in the secondary structures?, and *4*) how do solvents influence the stabilities of secondary structures? In this paper, we would like to report a theoretical study on a series of poly-β-alanine models to address the above questions. In addition, our results will provide valuable information for the calibration of molecular mechanics force fields.

2. Results and Discussion. – *Calculation Strategy and Methodology.* A β-strand that forms a β-sheet with another strand is a linear structure not stabilized by *intra*molecular

H-bonds, in contrast to the other secondary structures shown above. Because our previous full geometry optimizations of β-hexapeptide models indicate that the middle residues tend to adopt a nearly identical repeating geometry [15][17], the present study employs a repeating-unit approach that has been successfully applied to the study of cooperative interactions in helical and sheet-type structures of α-peptides and sheets of β-peptides [21]. As shown in structure **A**, a peptide has n repeating units (residues). To derive the starting conformation of the repeating units for β-strand, *C6*-ribbon, 2_8-ribbon, *10*-helix, *12*-helix, and *14*-helix, Ac-(β-Ala)$_5$-NH$_2$ was optimized with the HF/6-31G* method and the GAUSSIAN 98 program [22], with a constraint of every amino acid residue in the same geometry. The same method was applied in the case of the *10/12*-helix, but a hexapeptide ($n=6$) model was used due to the 10-m-r and 12-m-r alternation. These repeating units were then used to build Ac-(β-Ala)$_n$-NH$_2$ ($n=0-9$), and the relative energies of 70 structures were calculated with the B3LYP/6-31G** method [23]. We have shown that these methods satisfactorily predict the conformational features of β- and oxa-peptides [6][15][17][24]. Finally, the solvation effects of MeOH on the conformational stabilities of these peptide models were evaluated by the SCIPCM approach [25].

Geometry. In *Fig. 1*, fragments of seven calculated secondary structures of β-peptides are shown. Selected geometrical parameters are given in *Table 1*. The *C6*-ribbon has a long O$\cdots$H(N) distance of 2.35 Å, but a very small O$\cdots$H–N angle of 103°, which prevents strong H-bonding. Each residue is rotated by *ca.* 240°, and *ca.* 1.5 residues finish one turn. 2_8-Ribbons are very similar to *C6*-ribbons, but they are conformationally more flexible and possess stronger H-bonds. The β-strand has all its C=O groups on one side, each residue spanning *ca.* 5 Å. However, the C=O groups are not perfectly parallel but slightly convex. This is due to the fact that the O=C–C$_\alpha$ and O=C–N angles make up *ca.* 122.5°, while the C$_\alpha$–C–N angles are only *ca.* 115° [21c]. The *10*/*12*-helix is characterized by alternate 10-m-r and 12-m-r H-bonded structures and features alternating 'up and down' dipoles. Therefore, *10*/*12*-helices possess small dipole moments (*Table 2*). The 12-m-r form has a larger O$\cdots$H–N angle (163°) than the 10-m-r (138°). The former is, thus, expected to be somewhat more stable than the latter. The 10-m-r form in the *10*-helix is different from that in the *10*/*12*-helix. The three dihedral angles ϕ, μ, ψ and are all positive (74°, 51°, and 74°, resp.). Compared to the *14*-helix, the *12*-helix displays shorter O$\cdots$H(N) distances and larger O$\cdots$H–N angles. As shown in *Table 1*, the calculated dihedral angles for these structures are quite close to those of fully-optimized structures reported before [15–17]. The calculated geometrical parameters for the *12*- and *14*-helices are in close agreement with reported X-ray crystal structures [2a,b].

Relative Stabilities. The calculated total dipole moments and relative stabilities of seven types of secondary structures of β-peptides are collected in *Table 2*. In *Fig. 2*, the calculated relative energies ΔE with respect to the *C6*-ribbon structure are plotted against the number of residues (n). Several features are apparent. *1*) In agreement with previous results, the *C6*-ribbon conformation is the most stable when $n=1-2$ [15–17]. *2*) The 2_8-ribbon energy runs almost parallel and close to that of *C6*. *3*) The relative energy of the β-strand linearly increases with respect to the *C6*-ribbon. Each unit of the former is *ca.* 6 kcal/mol less stable than that in the latter. Such a large destabilization is apparently due to repulsions between neighboring dipoles. *4*) The *12*-helical structure is

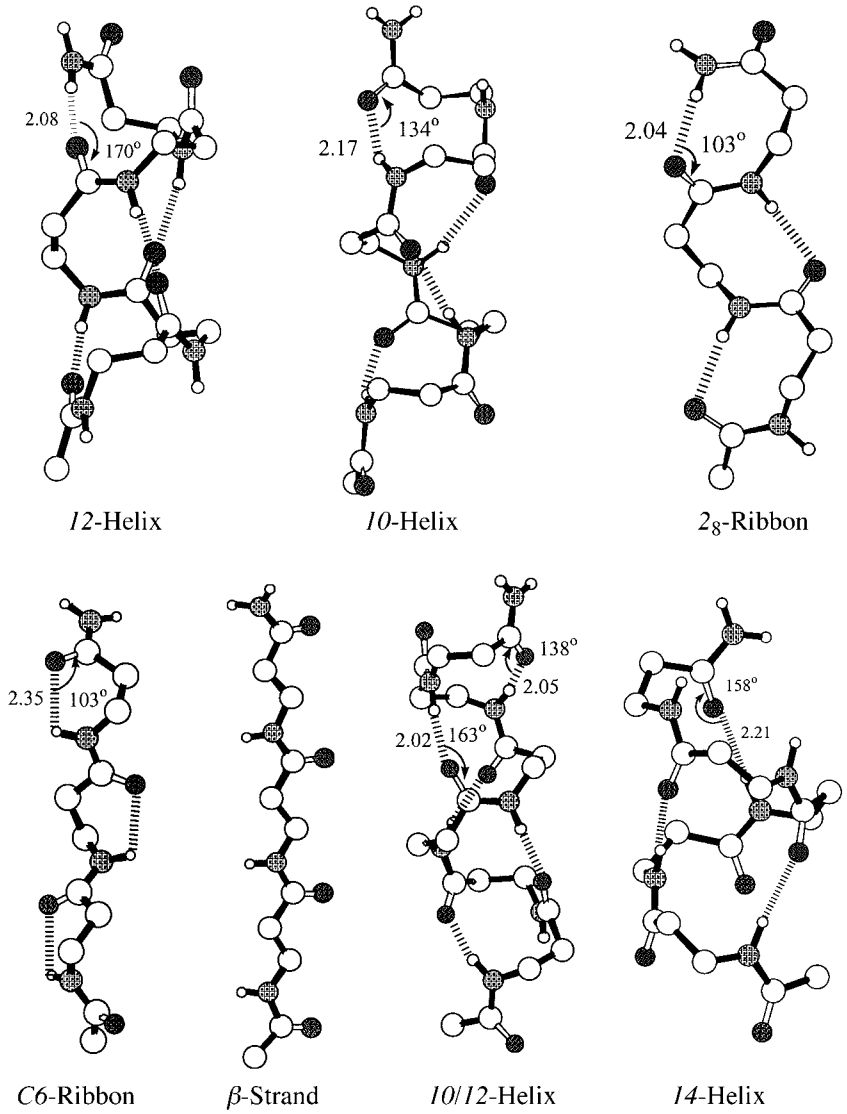

Fig. 1. *Fragments of calculated secondary structures of poly-β-alanine*

ca. 6 kcal/mol higher in energy than the *C6*-ribbon for $n=1$, but is gradually stabilized when n is increased, reaching the stability of the *C6*-ribbon when n becomes 7. *5*) The *14*-helix is very unstable for short peptides. It is *ca*. 10 kcal/mol less stable than the *C6*-ribbon for a model tripeptide ($n=3$). However, when n becomes larger, its stability rapidly increases. Our prediction is that it will catch up to the stability of the *C6*-ribbon at $n=10$. In the gas phase, the *12*- and *10*-helices are predicted to be more stable than the *14*-helix by *ca*. 6–8 and 8–10 kcal/mol, respectively. As will be shown later, this

Table 1. *Calculated Geometrical Parameters for β-Peptide Secondary Structures* (*cf. Fig. 1*)

Structure	Residues/turn	Rise [Å]	Pitch [Å]	Φ	μ	Ψ
C6-ribbon	1.7	4.0	6.8	99.2	62.9	175.8
β-strand	–	4.9	–	180.0	180.0	180.0
10/*12*-helix	2.7	2.1	5.7	– 99.3/89.5	61.3/65.9	89.9/ – 110.6
14-helix	3.1	1.7	5.2[a])	– 141.6	59.9	– 133.3
12-helix	2.7	2.2	5.9[b])	– 88.5	89.3	– 111.4
10-helix	2.6	2.3	6.0	73.5	51.3	73.6
2_8-ribbon	2.2	3.0	6.7	– 111.5	68.6	13.9

[a]) Exper. value: 5.0 Å. [b]) Exper. value: 5.6 Å.

situation changes in MeOH solution. *6*) For peptides with more than two residues, the *10*/*12*-helix is the most stable. The preference of this helical structure over the other secondary structures increases significantly when the peptide becomes longer. This clearly indicates a very large intrinsic preference of *β*-peptides to adopt the *10*/*12*-helical structure in the gas phase, in agreement with earlier conclusions [17].

Cooperative Residue Energy. It is expected that, in different secondary structures, amino acid residues undergo different interactions, which are vital for the relative stabilities of these elements. We calculated the residue energy $\varepsilon_n = E(n) - E(n-1)$ corresponding to the incremental energy difference between a peptide with n residues and its $n-1$ homologue. These residue energies are listed in *Table 3*.

In each secondary structure, each residue is geometrically the same and, therefore, experiences similar steric effects (*cf. Fig. 6*). Therefore, the variation of the residue energy reflects electrostatic interactions among the residues in a given secondary

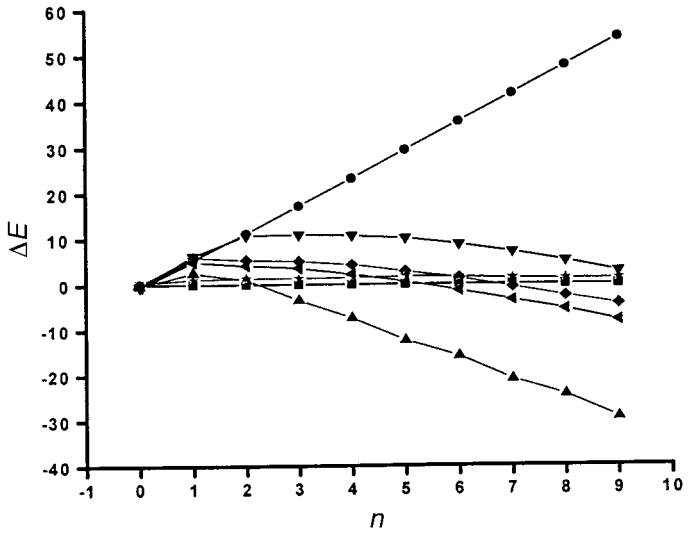

Fig. 2. *Plot of total relative energies* ΔE [kcal/mol] *of the* C6-*ribbon* (■), *β-strand* (●), 10/12-*helix* (▲), 14-*helix* (▼), 12-*helix* (◆), 10-*helix* (◀), *and* 2_8-*ribbon* (★) *models calculated with the B3LYP/6-31G** method*

Table 2. *Total Dipole Moments and Relative Energies of the* C6-*Ribbon* (A), *β-Strand* (B), 10/12-*Helix* (C), 14-*Helix* (D), 12-*Helix* (E), 10-*Helix* (F), *and* 2_8-*Ribbon* (G) *Structures Calculated by the B3LYP/6-31G** Method*

n	Dipole Moment [D]						
	A	B	C	D	E	F	G
0	3.8	3.7	3.8	3.7	3.6	3.8	3.7
1	4.2	7.1	3.4	6.9	5.8	5.8	4.7
2	7.2	10.5	6.7	10.1	9.6	9.0	8.0
3	9.2	13.8	5.1	14.2	13.5	12.8	10.5
4	11.8	17.1	7.4	18.6	17.3	16.3	13.6
5	14.4	20.2	3.7	23.0	21.6	20.3	16.5
6	16.8	23.2	6.2	27.6	25.8	24.3	19.6
7	19.5	26.0	1.5	32.4	30.0	28.3	22.7
8	21.8	28.7	6.2	37.1	34.4	32.4	25.7
9	24.6	31.1	4.1	42.0	38.6	36.5	28.2
	Relative Energy [kcal/mol]						
	A	B	C	D	E	F	G
0	0	– 0.1	– 0.2	– 0.3	0.2	– 0.4	0.3
1	0	5.4	2.6	6.2	6.0	5.0	1.3
2	0	11.3	1.1	10.8	5.4	4.2	1.5
3	0	17.3	– 3.4	11.0	5.1	3.6	1.5
4	0	23.3	– 7.3	10.7	4.3	2.2	1.6
5	0	29.5	– 12.4	10.1	2.8	0.7	1.7
6	0	36.8	– 15.8	8.7	1.4	– 1.4	1.6
7	0	41.8	– 20.9	7.1	– 0.6	– 3.4	1.3
8	0	47.9	– 24.4	5.1	– 2.6	– 5.5	1.3
9	0	54.1	– 29.3	2.8	– 4.3	– 8.0	1.3

structure. Assuming that residue n only interacts with residue $n-1$, but not with residues $<(n-1)$, then the residue energy should be constant since there is no cooperativity within such a secondary structure. However, if residue n interacts with remote residues, then the residue energy should vary with n. When ε_n becomes more negative with increasesing n, it means that the additional amino acid residue cooperatively interacts with remote residues, which results in a stabilization of the secondary structure. The term $\varepsilon_n - \varepsilon_{n-1}$ roughly represents the interaction between the two terminal residues and should approach zero when n becomes very large.

The residue energies for the seven types of secondary structures are shown in *Fig. 3*. The residue energy is almost constant for the *C6*-ribbon, 2_8-ribbon, and β-strand, indicating no electronic interaction between any two remote residues. As expected, there is a large stabilization of *ca.* 4–6 kcal/mol for ε_2 relative to ε_1 for the *10*-helix, *12*-helix, and the *10*/*12*-helix, as well as for ε_3 relative to ε_2 for the *14*-helix. This is attributed to the formation of the first H-bond for these helical structures. Interestingly, ε_n continues to increase (in a negative sense) with increasing n for the *10*-helix, *12*-helix, and *14*-helix. It reaches a maximum for the *10*-helix and *12*-helix near $n=7$. However, for the *14*-helix, even when n reaches 9, the residue energy still increases. This means that single residues still electronically interact in the gas phase although being separated by *ca.* 16 Å.

Table 3. *Calculated Residue Energy* ε_n *and Residue Dipole Moment in the* C6-*Ribbon* (A), *β-Strand* (B), 10/12-*Helix* (C), 14-*Helix* (D), 12-*Helix* (E), 10-*Helix* (F), *and* 2_8-*Ribbon* (G) *Structures of β-Peptide Models Calculated with the B3LYP/6-31G** Method*

n	Residue Energy [kcal/mol]						
	A	B	C	D	E	F	G
1	−7.1	−1.5	−4.2	−0.5	−1.3	−1.7	−6.1
2	−6.9	−1.1	−8.5	−2.4	−7.5	−7.7	−6.7
3	−7.2	−1.2	−11.7	−7.0	−7.4	−7.8	−7.2
4	−7.1	−1.2	−11.1	−7.4	−8.0	−8.5	−7.1
5	−7.3	−1.1	−12.3	−7.9	−8.8	−8.8	−7.1
6	−7.3	−1.1	−10.7	−8.6	−8.9	−9.3	−7.4
7	−7.3	−1.1	−12.4	−9.0	−9.3	−9.3	−7.5
8	−7.3	−1.2	−10.8	−9.3	−9.4	−9.3	−7.4
9	−7.3	−1.1	−12.2	−9.6	−9.6	−9.7	−7.3
	Residue Dipole Moment [D]						
	A	B	C	D	E	F	G
1	4.0	3.5	3.7	3.3	3.4	3.5	4.3
2	4.1	3.5	4.6	3.4	4.3	4.2	4.3
3	4.1	3.6	4.7	4.3	4.4	4.4	4.4
4	4.1	3.6	4.7	4.5	4.5	4.5	4.5
5	4.2	3.6	4.8	4.6	4.6	4.6	4.5
6	4.2	3.6	4.8	4.8	4.7	4.7	4.5
7	4.2	3.6	4.8	4.9	4.7	4.7	4.5
8	4.2	3.6	4.8	5.0	4.8	4.7	4.5
9	4.2	3.6	4.9	5.0	4.8	4.8	4.5

The residue energy of the *10*/*12*-helix displays a zigzag pattern after $n = 3$. This is due to the difference between 10-m-r H-bonded and 12-m-r H-bonded structures. Our earlier gas-phase calculations of Ac-(β-Ala)$_2$-NH_2 indicated that the 12-m-r form is *ca.* 1.7 kcal/mol more stable than the 10-m-r form. Thus, between odd and even numbered peptides, there is an energy difference of *ca.* 1.5 kcal/mol. Furthermore, it appears that large cooperative interactions occur within a short range of *ca.* 4 residues, but essentially none beyond this range. Thus, the formations of the *10*-, *12*-, and *14*-helices are cooperative in the gas phase. For the *10*-helix and *12*-helix, the 9th residue is *ca.* 2.1 kcal/mol more stable than the 2nd residue. For the *14*-helix, the 9th residue is more stable than the 3rd residue by *ca.* 2.6 kcal/mol. Once the first H-bond is formed, the energy differences between the *10*- and *12*-helix, or the *12*- and *14*-helix are nearly constant, one being worth *ca.* −1.0 kcal/mol, the other −2.8 kcal/mol. These results suggest that those secondary structures that formally contain mono 'rings' interact in a similar way. Thereby, 'ring' size probably determines the spatial arrangement of polar groups. Please notice that ε_2 of the *14*-helix is *ca.* 2.4 kcal/mol more negative than ε_1. This indicates that there is a large inductive stabilizing interaction between the first and third dipoles (residues i, $i+2$), which are nearly parallelly oriented. We conclude that cooperative long-range electrostatic interactions play a crucial role in the formation of these helices, no matter whether H-bonds are involved or not.

Origin of Cooperative Residue Energy. To further understand the nature of the cooperative residue energy, we analyzed the incremental change in dipole moment as a

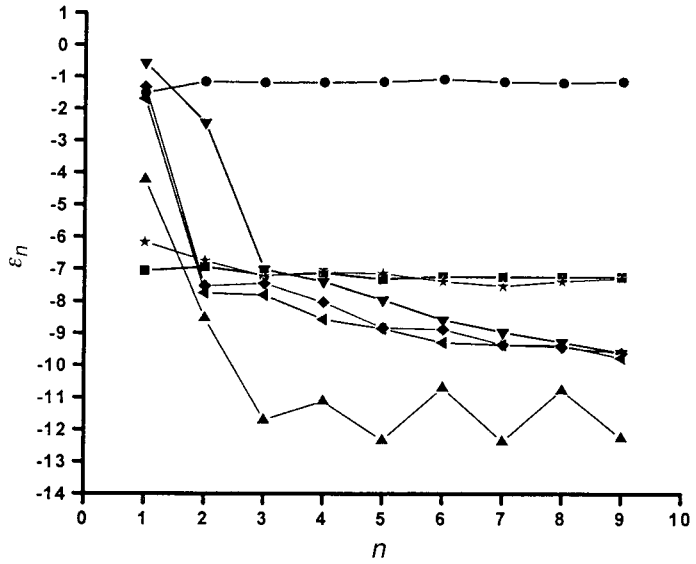

Fig. 3. *Plot of residue energies* ε_n [kcal/mol] *of the* C6-*ribbon* (■), *β-strand* (●), 10/12-*helix* (▲), 14-*helix* (▼), 12-*helix* (◆), 10-*helix* (◀), *and* 2_8-*ribbon* (★) *models calculated with the B3LYP/6-31G** method*

function of *n*. The residue dipole moment of the *n*th residue is calculated by the vector subtraction of the dipole moment of the $n-1$ model peptide from that of the model peptide *n*. These values are listed in *Table 3*. As shown in *Fig. 4*, the residue dipole moments of the *β*-strand, 2_8-ribbon, and *C6*-ribbon are nearly constant. However, the residue dipole moments of the *10*-helix, *12*-helix, and *14*-helix increase as *n* increases. In the case of the *14*-helix, the residue dipole moment increases by *ca.* 60% for $n = 1 \rightarrow 9$ (*Table 3*). The calculated dipole moment of acetamide is *ca.* 3.8 D, which can be considered as the intrinsic dipole moment of a peptide amino acid residue. Deviations of the calculated residue dipole moments are due to induced dipoles, which reflects electrostatic interactions between residues. That is, a stabilizing interaction tends to amplify itself by inducing a positive dipole, while a destabilizing interaction tends to reduce itself by inducing an opposite dipole. The calculated residue dipole moment of the *β*-strand (3.6 D) is smaller than that of acetamide by *ca.* 0.2 D, reflecting the repulsive nature of interactions between neighboring residues $(i, i+1)$. The residue dipole of the *C6*-ribbon is *ca.* 4.1 D and results from a small attractive interaction between two neighbors. The residue dipole of the 2_8-ribbon is larger than that of the *C6*-ribbon, which is in agreement with the fact that the 2_8-ribbon forms stronger H-bonds. The formation of H-bonds in the four helical structures, *10*-, *12*-, *14*-, and *10*/*12*-helices, results in a large stabilization accompanied by large induced dipoles. Therefore, there is a fair correlation between calculated residue energies and residue dipole moments: The *C6*-ribbon, 2_8-ribbon, and *β*-strand possess nearly constant residue energies and residue dipole moments, while the *10*-, *12*-, and *14*-helices give rise to continuously increasing residue energies and residue dipole moments as the peptide elongates. The *10*/*12*-helix is characterized by a large cooperative residue energy on a short range of *ca.* 4 residues.

The *14*-helix displays the most significant induced residue dipole moment and the largest cooperativity in the gas phase. Cooperative interactions in the *10*-, *12*-, and *14*-helices are mainly due to long-range electrostatic interactions.

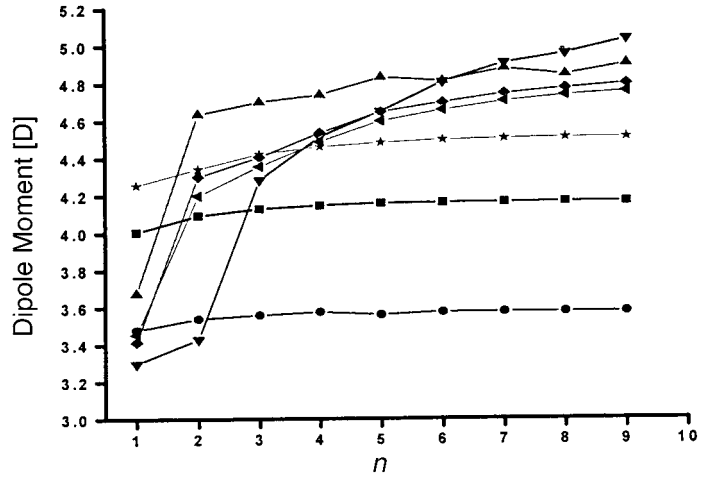

Fig. 4. *Residue dipole moment of the* C6*-ribbon* (■), *β-strand* (●), 10/12*-helix* (▲), 14*-helix* (▼), 12*-helix* (◆), 10*-helix* (◀), *and* 2_8*-ribbon* (★) *models calculated with the B3LYP/6-31G** method*

What is the mechanism for the cooperative residue energy or long-range interaction? One possible mechanism is the 'through-bond' cooperative formation of H-bonds [26]. In the *C6*-ribbon and 2_8-ribbon, there is one such network, and in the other four helical structures, there are two H-bonding networks. It has been proposed that contiguous H-bonds might cause a resonance-type stabilization [27], that is, H-bonds reinforce each other. However, in a series of calculations, we found that ribbon structures that are held together by H-bonds between neighboring residues do not possess cooperative residue energies. Thus, the 2_7-ribbon of α-peptides [21], the *C6*- and 2_8-ribbons of β-peptides, and the *9*-helix (or 2_9-ribbon) of γ-peptides [28] all have nearly constant residue energies. Therefore, our calculations do not support the above explanation – at least in these intramolecularly hydrogen-bonded systems. Another explanation for the cooperative forces is based on through-space dipole-dipole interactions. This has been recognized for α-peptides [29]. As a matter of fact, long-range electrostatic interaction is an important part of currently widely used molecular mechanics force-fields [30][31]. We have repeated the above calculations using the popular *MacroModel* program [32]. Although very different results were generated with different force-fields, cooperative interactions in helical structures were always found. However, these force-fields, which are based on fixed atomic charges or bond dipole moments, often tend to overexpress the cooperative residue energy in short range interactions (within 6 residues), but underestimate long range interactions, observed, *e.g.*, in α-peptides [21][33]. Therefore, induced electrostatic interactions, which are qualitatively represented by induced dipoles, are needed for the improvement of these force-fields.

To further support the importance of through-space-induced dipoles with respect to cooperativity, we studied the conformational preference of polyketones of type **B** [34]. While the α-helical structure of **B** is quite similar to the peptide α-helix in terms of backbone conformation, here, no H-bond is possible. Nevertheless, a considerable cooperativity was derived for the formation of the α-helical structure [35]. There was also a high correlation between calculated residue energies and residue dipole moments. It is, thus, possible that such cooperative long-range electrostatic interactions are important for the helical structure formation of other polymeric materials [36][37].

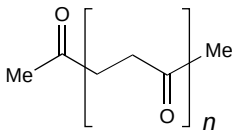

B

Separation of Electrostatic and Torsional Effects. To better understand the interactions among residues in each secondary structure, we attempted to separate the residue electrostatic effect and torsional effect based on the strategy shown in the *Scheme*. A monopeptide model compound shall serve as an example ($n=1$). Starting from a given secondary structure with an electrostatic energy E, the two CH_2 groups are replaced by two H-atoms, so that the peptide model breaks into two amides units (*Step 1*). This removes the torsional interactions of the $(CH_2)_2$ linker, while the electrostatic interaction between the two detached amide units persists. When the two amides are separated to an infinite distance (*Step 2*), the electrostatic interaction is also removed. The energy difference between E' (*Step 1*) and E'' (*Step 2*) should reflect the electrostatic interaction (E_{elec}) between the two amide units. In reality, the distance between the two H-atoms is quite short (*ca.* 2 Å) and not constant in different secondary structures. Therefore, the above electrostatic interactions should be corrected by the steric interaction (E_{corr}) of the two H-atoms. In principle, the two amide units also sterically interact. However, that contribution is probably negligible.

For longer model peptides, *e.g.*, $n=3$, three $(CH_2)_2$ groups have to be replaced by H-atoms to generate four amide units, and the total electrostatic interaction can be derived in a similar way, $E_{elec}(n)=E'(n)-E''(n)-E_{corr}$. Just like the calculations of residue energies, residue electrostatic interactions can be derived from the total electrostatic interactions of model peptides: $\varepsilon_{elec}(n)=E_{elec}(n)-E_{elec}(n-1)$. In *Fig. 5*, the calculated residue electrostatic interactions are depicted. Several points are interesting. *1*) The calculated variations of residue energies for the seven secondary structures are essentially the same as the calculated residue energies. This confirms that the variation in residue energy for each secondary structure is due to electrostatic interactions. *2*) For the β-strand, each residue electrostatic interaction makes up *ca.* 0.6 kcal/mol, which corresponds to an electrostatic repulsion between neighboring, roughly parallel amide dipoles. *3*) There is a significant stabilizing electrostatic interaction (*ca.* 5–6 kcal/mol) between the two neighboring amino acid residues in the *C6*- and 2_8-ribbon structure. *4*) The *10*-helix, *12*-helix, and *10/12*-helix profit considerably from larger residue electrostatic stabilizations than the *C6*-ribbon and the *14*-helix. The *10*/*12*-helix displays the largest residue electrostatic interaction.

Scheme

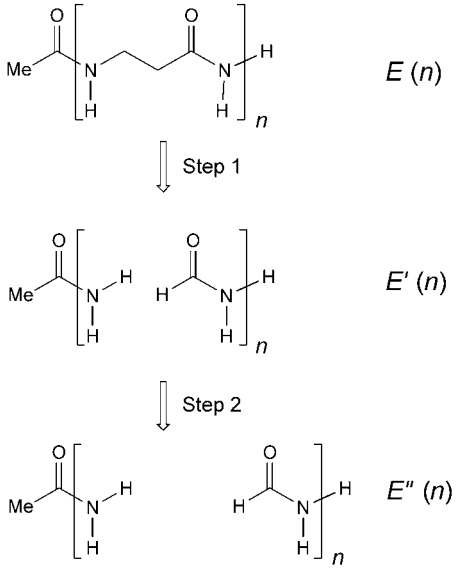

Total electrostatic energy:
$E_{elec}(n) = E'(n) - E''(n) - E_{corr}$

Residue electrostatic energy:
$\varepsilon_{elec}(n) = E_{elec}(n) - E_{elec}(n-1)$

Residue steric energy:
$\Delta E_{steric}(n) = \Delta E(n) - \Delta E_{elec}(n)$

$\Delta E(n)$:
Relative energy of the *C6*-ribbon structure according to *Table 2*

$\Delta E_{elec}(n)$:
Relative electrostatic energy with respect to the *C6*-ribbon structure (*cf. Fig. 5*)

E_{corr}:
Steric interaction energy between two pairs of H-atoms

5) The *14*-helix suffers from a destabilizing electrostatic residue energy for the first and second residues. That is, the *i*th residue undergoes repulsive interactions with the $(i+1)$th and $(i+2)$th residues, which partly explains the instability of the 14-helix in the gas phase. *6*) The strength of the first H-bond in the *10*-helix, *12*-helix, *14*-helix, and *10*/*12*-helix is *ca.* 4–4.5 kcal/mol [38].

The torsional interaction, or steric effect, can only be estimated on a relative basis. Since the relative stabilities of the secondary structures are the sum of electrostatic and torsional contributions, the torsional energies can be derived by subtracting the relative electrostatic energies $\Delta E_{elec}(n)$ from the total relative energies $\Delta E(n)$. *Fig. 6* depicts the derived torsional interactions with respect to the *C6*-ribbon structure. The torsional energy changes linearly with n, except for the *10/12*-helix (alternating 10-m-r and 12-m-r structures). Since the relative residue torsional energies correspond to the slopes of these lines, the following conclusions can be drawn. *1*) The *C6*-ribbon and β-strand possess similar torsional interactions. *2*) The *12*-helix is sterically destabilized by *ca.* 0.6 kcal/mol per residue relative to the C6-ribbon. The *12*-helix has a dihedral angle μ of *ca.* 90°. Thus, the C–C bond is partially eclipsed. In addition, the acetamide unit itself in the *12*-helix is distorted to some extent so that it causes a small destabilization. As shown in *Table 2*, the acetamide unit ($n=0$) in the *12*-helix is *ca.* 0.5 kcal/mol less stable than in the *14*-helix. *3*) The *14*-helix is in a perfect *gauche* conformation (C_α–C_β bond, dihedral angle μ). Therefore, the torsional energies of *10*-helix, *10*/*12*-helix, and *14*-helix are directly related to deviations from ideal dihedral angles μ. When μ is smaller than 60°, two acetamide units are relatively close to each other, which leads to a destabilization. This is in full agreement with *Seebach*'s assessment that staggered μ dihedral angles partly explain the occurrence of the *14*-helix [39].

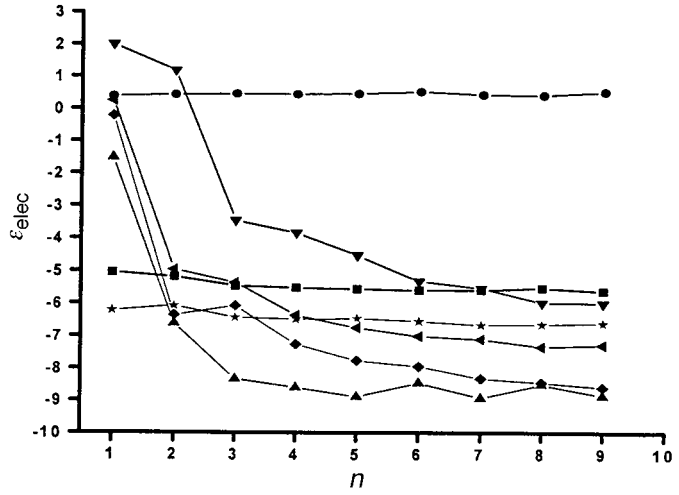

Fig. 5. *Plot of residue electrostatic energies* ε_{elec} [kcal/mol] *of the* C6-*ribbon* (■), *β-strand* (●), 10/12-*helix* (▲), 14-*helix* (▼), 12-*helix* (◆), 10-*helix* (◀), *and* 2_8-*ribbon* (★) *models calculated with the B3LYP/6-31G** method*

Solvent Effects. The identification of residue electrostatic interactions allows a qualitative prediction of non-aqueous polar-solvent effects on the stabilities of secondary structures. The *10*/*12*-, *10*-, and *12*-helices, which benefit most from electrostatic interactions, should be stabilized to a greater extent by polar solvents than the *14*-helix, which has a much smaller residue electrostatic interaction than the

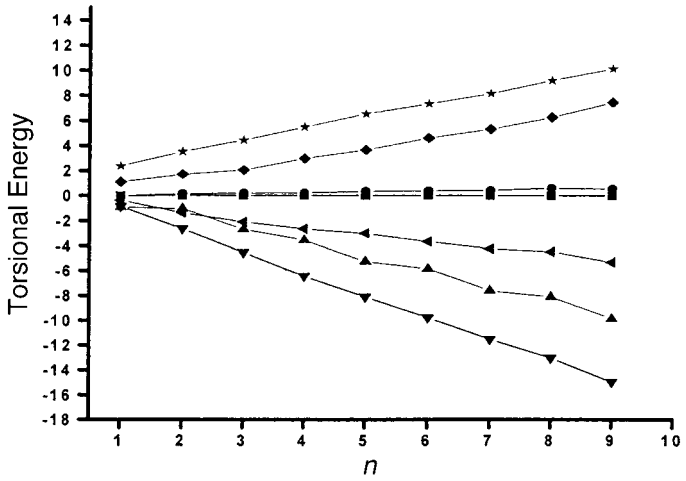

Fig. 6. *Plot of total torsional energies* vs. *the number of β-Ala residues* (*n*) [kcal/mol] *of the* C6-*ribbon* (■), *β-strand* (●), 10/12-*helix* (▲), 14-*helix* (▼), 12-*helix* (◆), 10-*helix* (◀), *and* 2_8-*ribbon* (★) *structures calculated with the B3LYP/6-31G** method*. The relative residue torsional energies are: *C6*-ribbon (0); *β*-strand (0); *10*/*12*-helix (−1.0 kcal/mol); *14*-helix (−1.5 kcal/mol); *12*-helix (0.6 kcal/mol); *10*-helix (−0.5 kcal/mol); 2_8-ribbon (0.6 kcal/mol).

12-helix. The β-strand, which suffers from a small electrostatic repulsion between nearly parallel C=O dipoles and which has a larger polar surface area than the helical structures, is expected to be strongly stabilized by polar organic solvents. All these predictions are based on SCIPCM solvent model calculations. *Fig. 7* depicts the calculated total solvation energies of the seven secondary structures in MeOH. The β-strand and the *14*-helix display the largest solvation energies, the *10*/*12*-helix the least. Interestingly, the 2_8-ribbon, *10*-helix, and *12*-helix are found to possess somewhat larger solvation energies than the *C6*-ribbon. This is in accord with the magnitudes of the dipole moments of the three structures (*cf. Table 2*).

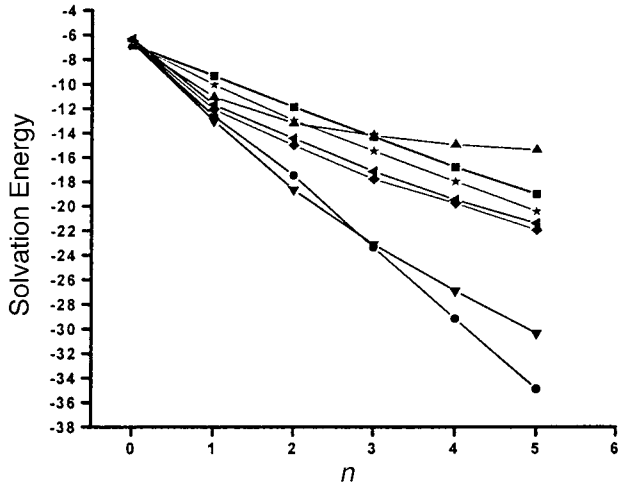

Fig. 7. *Plot of total solvation energies* [kcal/mol] *of the* C6-*ribbon* (■), *β-strand* (●), 10/12-*helix* (▲), 14-*helix* (▼), 12-*helix* (◆), 10-*helix* (◀), *and* 2_8-*ribbon* (★) *models calculated with the B3LYP/6-31G** method* ($e = 33.0$ for MeOH, isosurface value = 0.0004)

The calculated total relative energies of the seven secondary structures in MeOH are listed in *Table 4* and plotted in *Fig. 8*. The *10*/*12*-helix is still the most stable structure for β-peptides with more than two residues. The β-strand is still the least stable, although solvent-stabilized. Interestingly, while the *12*-helix is more stable than the *14*-helix by *ca.* 6–8 kcal/mol in the gas phase, in MeOH, the *14*-helix becomes more stable for model peptides longer than 4 residues.

The calculated relative solvation energies in MeOH (*Fig. 7*) are all nearly linear for $n > 4$, indicating that the cooperativity effects for the helical structures nearly disappear in polar solvents. This is understandable, since the cooperativity for the helical structure is due to long-range electrostatic interactions, which are dominant in the gas phase but significantly reduced in polar solvents.

Recently, *Seebach* and co-workers studied temperature-dependent NMR and CD spectra of a β-hexa- and heptapeptide in MeOH [39]. Between 298 and 393 K, the peptides were found in the *14*-helix (3_{14}-helix) conformation. The authors suggested that the unfolding process is *stepwise* and not *cooperative*, as found in α-peptides [40]. Moreover, staggered conformations with respect to μ were proposed to be crucial for the *14*-helix. We would like to comment on this. In the case of α-peptides, there is a

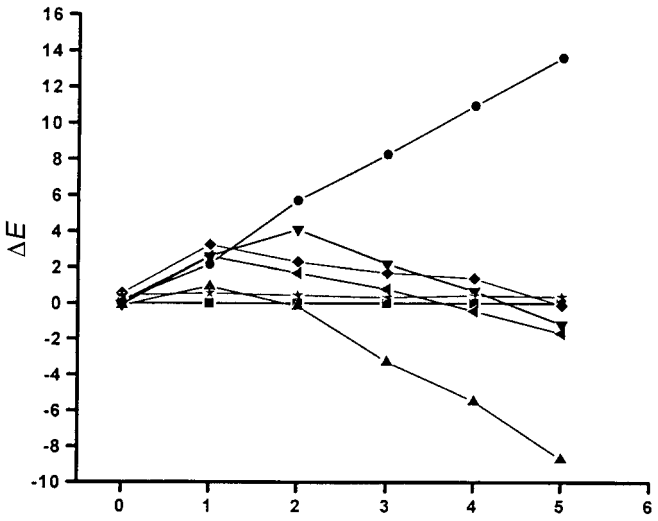

Fig. 8. *Plot of total relative energies* ΔE [kcal/mol] *in MeOH of the* C6-*ribbon* (■), β-*strand* (●), 10/12-*helix* (▲), 14-*helix* (▼), 12-*helix* (◆), 10-*helix* (◀), *and* 2_8-*ribbon* (★) *models calculated with the B3LYP/6-31G** method*

Table 4. *Calculated Solvation Energies and Total Relative Energies in MeOH of the* C6-*Ribbon* (A), β-*Strand* (B), 10/12-*Helix* (C), 14-*Helix* (D), 12-*Helix* (E), 10-*Helix* (F), *and* 2_8-*Ribbon* (G) *Structures Calculated with the B3LYP/6-31G** Method*

n	Solvation Energies (kcal/mol)						
	A	B	C	D	E	F	G
0	– 6.9	– 6.6	– 6.7	– 6.6	– 6.5	– 6.3	– 6.7
1	– 9.3	– 12.6	– 11.0	– 12.9	– 12.0	– 11.6	– 10.0
2	– 11.9	– 17.4	– 13.1	– 18.1	– 15.0	– 14.4	– 12.9
3	– 14.3	– 23.3	– 14.2	– 23.1	– 17.7	– 17.1	– 15.4
4	– 16.8	– 29.1	– 14.9	– 26.9	– 19.7	– 19.4	– 17.9
5	– 19.0	– 34.8	– 15.3	– 30.3	– 21.9	– 21.4	– 20.4
	Relative Energies (kcal/mol)						
	A	B	C	D	E	F	G
0	0	0.2	– 0.1	– 0.1	0.6	0.2	0.5
1	0	2.2	1.0	2.6	3.2	2.6	0.6
2	0	5.7	– 0.2	4.1	2.3	1.7	0.5
3	0	8.3	– 3.3	2.2	1.7	0.8	0.3
4	0	11.0	– 5.5	0.7	1.4	– 0.4	0.4
5	0	13.7	– 8.7	– 1.2	– 0.1	– 1.7	0.4

cooperative transition between *random coil* and *helical* structures [40]. Since the random coil state is entropically favored, the melting of α-helices is temperature-dependent. Our calculations indicate that the conformation corresponding to the 14-helix is the most stable in MeOH solution. This, however, seems to be partially due to a favorable entropy, which is approx. the same as in an extended conformation. The latter is not enthalpically but entropically favored by more than two entropy units relative to

other conformations. Therefore, the *14*-helix is most likely *not* in equilibrium with a random coil structure.

Our earlier calculations also suggest that the *14*-helix is favored over the *10*/*12*-helix for β^3-peptides, because the *14*-helix is not destabilized by β-substituents, while half of them have to take unfavourable positions in the *10*/*12*-helix (destabilization of *ca*. 3 kcal/mol per substituent [17]). It is not surprising that no melting is observed for the above two *Seebach* peptides. Since the *14*-helix has a somewhat larger entropy than the *10*/*12*-helix, a temperature increase slightly favors the *14*-helix.

Finally, our calculations suggest that the *14*-helix is significantly stabilized by polar solvents. Therefore, it will be interesting to see whether the *14*-helix of β^3-peptides can be converted to a *10*/*12*-helix when solvent polarity is reduced.

3. Summary. – Calculations of a series of Ac-(β-Ala)$_n$-NH_2 model peptides suggest that there is an intrinsic preference for the formation of a *10*/*12*-helix in the gas phase. Just like the α-helix of α-peptides, the formation of *10*-, *12*- and *14*-helices of β-peptides is characterized by a significant cooperative residue energy in the gas phase. There is an excellent correlation between calculated residue energy and residue dipole moment, indicating the importance of long-range electrostatic interactions. The dipole-induced cooperativity is not due to resonance-type interactions through H-bonded networks. Instead, it is mainly caused by through-space dipole-dipole interactions. By removing the $(CH_2)_2$ group of single residues, it is possible to separate electrostatic and torsional interaction in the secondary structures of β-peptides. The *10*/*12*-, *10*-, and *12*-helices benefit most from electrostatic interactions, while the *14*-helix is most favored in terms of torsional effects. Therefore, it is expected that solvent polarity plays an important role in the relative stabilities of secondary structures of β-peptides. Since substituents also strongly influence the stability of secondary structures, it will be interesting to carry out a systematic theoretical study in which different substituents are implemented.

This work was supported by the *Research Grants Council* of Hong Kong. *Y. D. W.* thanks the *Croucher Foundation* for a *Senior Research Fellowship* award.

REFERENCES

[1] D. Seebach, J. L. Matthews, *Chem. Commun*. **1997**, 2015; S. H. Gellman, *Acc. Chem. Res.* **1998**, *31*, 173; K. Gademann, T. Hintermann, J. V. Schreiber, *Curr. Med. Chem.* **1999**, *6*, 905; W. F. DeGrado, Y. Hamuro, *J. Peptide Res.* **1999**, *54*, 206; R. P. Cheng, S. H. Gellman, W. F. DeGrado, *Chem. Rev.* **2001**, *101*, 3219.

[2] a) D. H. Appella, L. A. Christianson, I. L. Karle, D. R. Powell, S. H. Gellman, *J. Am. Chem. Soc*. **1996**, *118*, 13071; b) D. H. Appella, L. A. Christianson, D. A. Klein, D. R. Powell, X. L. Huang, J. J. Barchi, S. H. Gellman, *Nature (London)* **1997**, *387*, 381; c) D. H. Appella, J. J. Barchi, S. R. Durell, S. H. Gellman, *J. Am. Chem. Soc*. **1999**, *121*, 2309; d) D. H. Appella, L. A. Christianson, I. L. Karle, D. R. Powell, S. H. Gellman, *J. Am. Chem. Soc*. **1999**, *121*, 6206; e) B. R. Huck, J. M. Langenhan, S. H. Gellman, *Org. Lett*. **1999**, *1*, 1717; f) J. D. Fisk, D. R. Powell, S. H. Gellman, *J. Am. Chem. Soc*. **2000**, *122*, 5443; g) X. F. Wang, J. F. Espinosa, S. H. Gellman, *J. Am. Chem. Soc*. **2000**, *122*, 4821; h) Y. J. Chung, B. R. Huck, L. A. Christianson, H. E. Stanger, S. Krauthauser, D. R. Powell, S. H. Gellman, *J. Am. Chem. Soc*. **2000**, *122*, 3995; i) T. L. Raguse, J. R. Lai, P. R. LePlae, S. H. Gellman, *Org. Lett*. **2001**, *3*, 3963; j) H.-S. Lee, F. A. Syud, X.-F. Wang, S. H. Gellman, *J. Am. Chem. Soc*. **2001**, *123*, 7721.

[3] D. Seebach, M. Overhand, F. N. M. Kühnle, B. Martinoni, L. Oberer, U. Hommel, H. Widmer, *Helv. Chim. Acta* **1996**, *79*, 913; D. Seebach, P. E. Ciceri, M. Overhand, B. Jaun, D. Rigo, L. Oberer, U. Hommel, R. Amstutz, H. Widmer, *Helv. Chim. Acta* **1996**, *79*, 2043; D. Seebach, S. Abele, K. Gademann, G. Guichard, T. Hintermann, B. Jaun, J. Matthews, J. V. Schreiber, *Helv. Chim. Acta* **1998**, *81*, 932; D. Seebach, K.

Gademann, J. V. Schreiber, J. L. Matthews, T. Hintermann, B. Jaun, L. Oberer, U. Hommel, H. Widmer, *Helv. Chim. Acta* **1997**, *80*, 2033; T. Hintermann, K. Gademann, B. Jaun, D. Seebach, *Helv. Chim. Acta* **1998**, *81*, 983; D. Seebach, S. Abele, S. Thjierry, M. Hanggi, S. Gruner, P. Seiler, *Helv. Chim. Acta* **1998**, *81*, 2218; S. Abele, P. Seiler, D. Seebach, *Helv. Chim. Acta* **1999**, *82*, 1559; T. Sifferlen, M. Rueping, K. Gademan, B. Jaun, D. Seebach, *Helv. Chim. Acta* **1999**, *82*, 2067; S. Abele, K. Vogtli, D. Seebach, *Helv. Chim. Acta* **1999**, *82*, 1539; T. Siggerlen, M. Rueping, K. Gademann, B. Jaun, D. Seebach, *Helv. Chim. Acta* **1999**, *82*, 2067; S. Abele, D. Seebach, *Eur. J. Org. Chem*. **2000**, *1*, 1; D. Seebach, A. Jacobi, M. Rueping, K. Gademann, M. Ernst, B. Jaun, *Helv. Chim. Acta* **2000**, *83*, 2115; P. I. Arvidsson, M. Rueping, D. Seebach, *Chem. Commun.* **2001**, 649; H. C. Le, T. Hintermann, T. Wessels, Z.-H. Gan, D. Seebach, R. R. Ernst, *Helv. Chim. Acta* **2001**, *84*, 208; D. Seebach, M. Rueping, P. I. Arvidsson, T. Kimmerlin, P. Micuch, C. Noti, D. Langenegger, D. Hoyer, *Helv. Chim. Acta* **2001**, *84*, 3503; K. Gademann, D. Seebach, *Helv. Chim. Acta* **2001**, *84*, 2924.

[4] J. M. Fernández-Santin, J. Aymamí, A. Rodríguez-Galán, S. Muñoz-Guerra, J. A. Subirana, *Nature (London)* **1984**, *311*, 53; C. Alemán, J. J. Navas; S. Muñoz-Guerra, *Biopolymers* **1997**, *41*, 721; M. García-Alvarez, A. Martínez de Ilarduya, S. León, C. Alemán, S. Muñoz-Guerra, *J. Phys. Chem. A* **1997**, *101*, 4215.

[5] B. W. Gung, D. Zou, Y. Miyahara, *Tetrahedron* **2000**, *56*, 9739; B. W. Gung, D. Zou, A. M. Stalcup, *J. Org. Chem*. **1999**, *64*, 2176; S. Hanessian, H. Yang, R. Schaum, *J. Am. Chem. Soc*. **1996**, *118*, 2507; T. D. W. Claridge, J. M. Goodman, A. Moreno, D. Angus, S. F. Barker, C. Taillefumier, M. P. Watterson, G. W. J. Fleet, *Tetrahedron Lett*. **2001**, *42*, 4251; R. P. Cheng, W. F. DeGrado, *J. Am. Chem. Soc*. **2001**, *123*, 5162; I. A. Motorina, C. Huel, E. Quiniou, J. Mispelter, E. Adjadj, D. S. Grierson, *J. Am. Chem. Soc*. **2001**, *123*, 8.

[6] A. K. Thakur, P. Venugopalan, R. Kishore, *J. Peptide Res.* **2000**, *56*, 55; S. A. Hopkins, J. P. Konopelski, M. M. Olmstead, H. D. Banks, *Tetrahedron* **2000**, 56, 9733; A. K. Thakur, P. Venugopalan, R. Kishore, *Biochem. Biophys. Res. Commun*. **2000**, *273*, 492; A. K. Thakur, R. Kishore, *Tetrahedron Lett*. **1999**, *40*, 5091.

[7] B. L. Iverson, *Nature (London)* **1997**, *385*, 113; *Chem. Eng. News* **1997**, *June 16*, 32; U. Koert, *Angew. Chem., Int. Ed*. **1997**, *36*, 1836.

[8] F. Schumann, A. Muller, M. Koksch, G. Muller, N. Sewald, *J. Am. Chem. Soc*. **2000**, *122*, 12009.

[9] D. Seebach, J. V. Schreiber, P. I. Arvidsson, J. Frackenpohl, *Helv. Chim. Acta* **2001**, *84*, 271; D. Seebach, T. Sifferlen, P. A. Mathieu, A. M. Hane, C. M. Krell, D. J. Bierbaum, S. Abele, *Helv. Chim. Acta* **2000**, *83*, 2849.

[10] T. Hintermann, D. Seebach, *Chimia* **1997**, *51*, 244; D. Seebach, S. Abele, J. V. Schreiber, B. Martinoni, A. K. Nussbaum, H. Schild, H. Schulz, H. Hennecke, R. Woessner, F. Bitsch, *Chimia* **1998**, *52*, 734.

[11] Y. Suhara, J. E. K. Hildreth, Y. Ichikawa, *Tetrahedron Lett*. **1996**, *37*, 1575; K. C. Nicolaou, H. Florke, M. G. Egan, T. A. Barth, V. A. Estevez, *Tetrahedron Lett*. **1995**, *36*, 1775.

[12] Y. Suhara, M. Izumi, M. Ichikawa, M. B. Penno, Y. Ichikawa, *Tetrahedron Lett*. **1997**, *38*, 7167; K. Gademann, M. Ernst, D. Hoyer, D. Seebach, *Angew. Chem., Int. Ed*. **1999**, *38*, 1223; K. Gademann, M. Ernst, D. Seebach, D. Hoyer, *Helv. Chim. Acta* **2000**, *83*, 16; K. Gademann, T. Kimmerlin, D. Hoyer, D. Seebach, *J. Med. Chem.* **2001**, *44*, 2460.

[13] N. Umezawa, M. A. Gelman, M. C. Haigis, R. T. Raines, S. H. Gellman, *J. Am. Chem. Soc*. **2002**, *124*, 368; E. A. Porter, X. F. Wang, H.-S. Lee, B. Weisblum, S. H. Gellman, *Nature (London)* **2000**, *404*, 565.

[14] S. Dedier, S. Krebs, J. R. Lamas, S. Poenaru, G. Folkers, J. A. L. de Castro, D. Seebach, D. Rognan, *J. Percept. Signal Transduct. Res.* **1999**, *19*, 645; S. Krebs, J. R. Lamas, S. Poenaru, G. Folkers, J. A. L. de Gastro, D. Seebach, D. Rognan, *J. Biol. Chem.* **1998**, *273*, 19072; D. Seebach, S. Poenaru, G. Folkers, D. Rognan, *Helv. Chim. Acta* **1998**, *81*, 1181; B. Gasslmaier, C. M. Krell, D. Seebach, E. Holler, *Eur. J. Biol.* **2000**, *267*, 5101; D. H. Liu, W. F. DeGrado, *J. Am. Chem. Soc*. **2001**, *123*, 7553.

[15] Y.-D. Wu, D.-P. Wang, *J. Am. Chem. Soc*. **1998**, *120*, 13485; Y.-D. Wu, D.-P. Wang, *J. Chin. Chem. Soc*. **2000**, *47*, 129.

[16] K. Mohle, M. Thormann, N. Sewald, H.-J. Hofmann, *Biopolymers* **1999**, *50*, 167; R. Günther, H.-J. Hofmann, K. Kuczera, *J. Phys. Chem. B* **2001**, *105*, 5559.

[17] Y.-D. Wu, D.-P. Wang, *J. Am. Chem. Soc*. **1999**, *121*, 9352.

[18] W. Damm, W. F. van Gunsteren, *J. Comput. Chem*. **2000**, *21*, 774; X. Daura, W. F. van Gunsteren, A. E. Mark, *Proteins* **1999**, *34*, 269; X. Daura, B. Jaun, D. Seebach, W. F. van Gunsteren, A. E. Mark, *J. Mol. Biol*. **1998**, *280*, 925; X. Daura, W. F. van Gunsteren, D. Rigo, B. Jaun, D. Seebach, *Chem.–Eur. J.* **1997**, *3*, 1410; X. Daura, K. Gademann, H. Schäfer, B. Jaun, D. Seebach, W. F. van Gunsteren, *J. Am. Chem. Soc*. **2001**, *123*, 2393.

[19] J. Aqvist, *FEBS Lett*. **1999**, *457*, 414; P. Bernadó, C. Alemán, J. Puiggalí, *Macromol. Theory Simul*. **1998**, *7*, 659.

[20] L. A. Christianson, M. J. Lucero, D. H. Appella, D. A. Klein, S. H. Gellman, *J. Comput. Chem*. **2000**, *21*, 763.
[21] a) Y.-D. Wu, Y.-L. Zhao, *J. Am. Chem. Soc*. **2001**, *123*, 5313; b) Y.-L. Zhao, Y.-D. Wu, *J. Am. Chem. Soc*. **2002**, *124*, 1570; c) Y.-D. Wu, J.-Q. Lin, S.-W. Luo, *J. Comput. Chem.*, in press.
[22] Gaussian 98 (Version A.7), *Gaussian*, Inc., Pittsburgh PA, 1998.
[23] A. D. Becke, *J. Chem. Phys.* **1993**, *98*, 5648; C. Lee, W. Yang, R. G. Parr, *Phys. Rev. B 37* **1988**, 785.
[24] Y.-D. Wu, D.-P. Wang, K. W. K. Chan, D. Yang, *J. Am. Chem. Soc*. **1999**, *121*, 11189; D. Yang, J. Qu, B. Li, F.-F. Ng, X.-C. Wang, K.-K. Cheugn, D.-P. Wang, Y.-D. Wu, *J. Am. Chem. Soc*. **1999**, *121*, 589; D. Yang, F.-F. Ng, Z.-J. Li, Y.-D. Wu, K. W. K. Chan, D.-P. Wang, *J. Am. Chem. Soc*. **1996**, *118*, 9794.
[25] K. B. Wiberg, T. A. Keith, M. J. Frisch, M. Murcko, *J. Phys. Chem*. **1995**, *99*, 9072; J. B. Forseman, T. A. Keith, K. B. Wiberg, J. Snoonian, M. J. Frisch, *J. Phys. Chem.* **1996**, *100*, 16098; J. Tomasi, R. Bonaccorsi, *Croat. Chem. Acta* **1992**, *12*, 69.
[26] G. A. Jeffrey, W. Saenger, 'Hydrogen Bonding in Biological Structures', Springer, Berlin, 1991.
[27] H. Guo, D. R. Salahub, *Angew. Chem., Int. Ed*. **1998**, *37*, 2985; H. Guo, M. Karplus, *J. Phys. Chem*. **1994**, *98*, 7104; B. W. Gung, Z. Zhu, *Tetrahedron Lett*. **1996**, *37*, 2189; B. W. Gung, Z. Zhu, B. Everingham, *J. Org. Chem*. **1997**, *62*, 3436.
[28] Y.-D. Wu, Y.-L. Zhao, unpublished results.
[29] A. Wada, *Adv. Biophys.* **1976**, *9*, 1; W. G. J. Hol, P. T. van Duijnen, H. J. C. Berendsen, *Nature (London)* **1978**, *273*, 443; D. A. Brant, *Macromolecules* **1968**, *1*, 291.
[30] MM2: N. L. Allinger, *J. Am. Chem. Soc*. **1977**, *89*, 8127. MM3: N. L. Allinger, Y. H. Yuh, J.-H. Lii, *J. Am. Chem. Soc*. **1989**, *111*, 8551; N. L. Allinger, L. Yan, *J. Am. Chem. Soc*. **1993**, *115*, 11918 and refs. cit. therein. AMBER3: S. J. Weiner, P. A. Kollman, D. T. Nguyen, D. A. Case, *J. Comput. Chem*. **1986**, *7*, 230. AMBER4: W. D. Cornell, P. Cieplak, C. I. Bayly, I. R. Gould, K. M. Merz Jr., D. M. Ferguson, D. C. Spellmeyer, T. Fox, J. W. Caldwell, P. A. Kollman, *J. Am. Chem. Soc*. **1995**, *117*, 5179. OPLS: W. L. Jorgensen, J. Tirado-Rives, *J. Am. Chem. Soc*. **1988**, *110*, 1657; W. L. Jorgensen, D. S. Maxwell, J. Tirado-Rives, *J. Am. Chem. Soc*. **1996**, *118*, 11225. MMFF: T. Halgren, *J. Comput. Chem.* **1996**, *17*, 490; T. Halgren, *J. Comput. Chem.* **1996**, *17*, 520; T. Halgren, *J. Comput. Chem.* **1996**, *17*, 553.
[31] D. E. Williams, in 'Reviews in Computational Chemistry', Eds. K. B. Lipkowiz, D. B. Boyd, Wiley, New York, 1991, Vol. 2, Chapt. 6; M. J. Dudek, J. W. Ponder, *J. Comput. Chem.* **1995**, *16*, 791.
[32] F. Mohamadi, N. G. J. Richards, W. C. Guida, R. Kiskamp, M. Lipton, C. Caufield, G. Chang, T. Hendrickson, W. C. J. Still, *Comput. Chem*. **1990**, *11*, 440.
[33] Detailed results and a modified force-field will be reported somewhere else.
[34] A. Sommazzi, F. Garbassi, *Prog. Polym. Sci*. **1997**, *22*, 1547.
[35] Y.-D. Wu, J.-M. Quan, unpublished results.
[36] K. Kirshenbaum, A. E. Barron, R. A. Goldsmith, P. Armand, E. K. Bradley, K. T. V. Truong, K. A. Dill, F. E. Cohen, R. N. Zuckermann, *Proc. Natl. Acad. Sci. U.S.A.* **1998**, *95*, 4303; P. Armand, K. Kirshenbaum, A. E. Barron, R. A. Goldsmith, S. Farr-Jones, A. E. Barron, K. T. V. Truong, K. A. Dill, D. A. Mierke, F. E. Cohen, R. N. Zuckermann, *Proc. Natl. Acad. Sci. U.S.A.* **1998**, *95*, 4309.
[37] R. B. Prince, J. G. Saven, P. G. Wolynes, J. S. Moore, *J. Am. Chem. Soc*. **1999**, *121*, 3114.
[38] G. A. Jeffrey, 'An Introduction to Hydrogen Bonding', Oxford University Press, N.Y., 1997.
[39] K. Gademann, B. Jaun, D. Seebach, R. Rerozzo, L. Scapozza, G. Folkers, *Helv. Chim. Acta* **1999**, *82*, 1.
[40] D. Poland, H. A. Scheraga, 'Theory of Helix-Coil Transitions in Biopolymers', Academic Press, N.Y., 1970.

Received June 5, 2002